Available online at www.sciencedirect.com
ScienceDirect
Journal of Organometallic Chemistry 691 (2006) 4304–4311
Journal of Organometallic Chemistry
www.elsevier.com/locate/jorganchem

Dinuclear hexamethylbenzene ruthenium cations containing η^1:η^2-2-(ferrocenyl)ethen-1-yl ligands: Synthesis, structure, electrochemistry

Mathieu J.-L. Tschan [a], Bruno Therrien [a], Jiří Ludvík [b], Petr Štěpnička [c,*], Georg Süss-Fink [a,*]

[a] Institut de Chimie, Université de Neuchâtel, Case Postale 158, CH-2009 Neuchâtel, Switzerland
[b] J. Heyrovský Institute of Physical Chemistry, Academy of Sciences of the Czech Republic, Dolejškova 3, CZ-18223 Prague, Czech Republic
[c] Charles University, Faculty of Science, Department of Inorganic Chemistry, Hlavova 2030, CZ-12840 Prague, Czech Republic

Received 9 May 2006; received in revised form 30 June 2006; accepted 7 July 2006
Available online 14 July 2006

Abstract

The cationic ferrocenyl-containing complexes $[(\eta^6\text{-}C_6Me_6)_2Ru_2(\mu\text{-}\eta^1\text{:}\eta^2\text{-}CH\text{–}CHFc)_2(\mu\text{-}H)]^+$ (**3**) and $[(\eta^6\text{-}C_6Me_6)_2Ru_2(\mu\text{-}PPh_2)(\mu\text{-}\eta^1\text{:}\eta^2\text{-}CH\text{–}CHFc)(\mu\text{-}H)]^+$ (**4**) have been synthesised in ethanol from ethynylferrocene and the dinuclear precursors $[(\eta^6\text{-}C_6Me_6)_2Ru_2(\mu\text{-}H)_3]^+$ (**1**) and $[(\eta^6\text{-}C_6Me_6)_2Ru_2(\mu\text{-}PPh_2)(\mu\text{-}H)_2]^+$ (**2**) respectively, and isolated as tetrafluoroborate salts. The spectroscopic data of **3** and **4** as well as the single-crystal X-ray diffraction analysis of [**4**][BF_4] show that the alkyne function of ethynylferrocene has been converted to a σ/π-ethenyl ligand by transfer of a bridging hydride from the diruthenium backbone onto the α-carbon of the triple bond in ethynylferrocene. The ferrocenyl-containing diruthenium compounds [**3**][BF_4] and [**4**][BF_4] as well as their parent compounds [**1**][BF_4] and [**2**][BF_4] have been studied by voltammetric techniques: Whereas **1** shows only an irreversible Ru(II)/Ru(III) oxidation, the phosphido-bridged derivative **2** displays two well-separated one-electron redox processes. In the case of **3** and **4**, the ferrocenyl substituents give rise to additional reversible ferrocene/ferrocenium waves.

Keywords: Arene ligands; Electrochemistry; Ferrocene derivatives; Phosphine ligands; Ruthenium

1. Introduction

Bimetallic complexes with a ruthenium centre and ferrocene-based ligands have been extensively studied as catalysts [1], electrochemical agents [2], electronic devices [3], and as molecular motors [4]. By contrast, only a few diruthenium complexes containing ferrocenyl [Fc = Fe(η^5-C_5H_4)(η^5-C_5H_5)] and ferrocene-1,1′-diyl [fc = Fe(η^5-C_5H_4)$_2$] moieties are known, $[Ru_2(\mu\text{-}OOCFc)_4(\eta^1\text{-}MeCH_2CH_2OH)_2][PF_6]$ [5], $[Ru_2(CO)_4(\mu\text{-}OOCFc)_2L_2]$ (L = NC_5H_5, PPh_3) [6], $[\{(\eta^6\text{-}C_6H_5(CH_2)_2OC(O)Fc)Ru(\mu\text{-}Cl)_2\}_2(\mu\text{-}fc(PPh_2)_2)]$ [7], $[Ru_2\{\mu\text{-}(NMe)_2CHPh\}_4(C{\equiv}CFc)_2]$ [8], $[Ru_2Cl(\mu\text{-}mpfa)_3\{\mu\text{-}(NMe)_2CH\text{-}C_6H_4\text{-}C{\equiv}CFc\}_2]$ (mpfa = *N*,*N*′-bis(*meta*-methoxyphenyl)formamidinate) [9], $[Ru_2\{\mu\text{-}(NMe)_2CH\text{-}C_6H_4\text{-}R\}_4(C_4Fc)_2]$ (R = H, OMe) [10], $[\{(\eta^5\text{-Cp})Ru(dppe)\}_2(\mu\text{-}\eta^1\text{:}\eta^1\text{-}(C{\equiv}C)_2fc)]$ [dppe = 1,2-bis(diphenylphosphino)ethane] [11] and $[(\eta^6\text{-}p\text{-}^i\text{PrMeC}_6H_4)_2Ru_2(\mu\text{-}S_2fc)(\mu\text{-}Cl)]^+$ [12]. Ethynylferrocene (ferrocenylacetylene) [13] can be used to introduce the ferrocenyl moiety into the diruthenium unit. However, in all ferrocenylethynyl-containing diruthenium complexes known, the ferrocenylethynyl ligand, FcC≡C, is coordinated as a terminal, one-electron σ-donor ligand to ruthenium [8,10]. A bridging three-electron η^1:η^2-coordination of FcC≡C to both ruthenium atoms of the dinuclear backbone has not yet been reported.

In recent years, we have shown that the trihydrido dinuclear cation $[(\eta^6\text{-}C_6Me_6)_2Ru_2H_3]^+$ possesses a great

* Corresponding authors. Tel.: +41 32 718 2405; fax: +41 32 718 2511.
E-mail addresses: stepnic@natur.cuni.cz (P. Štěpnička), georg.suess-fink@unine.ch (G. Süss-Fink).

0022-328X/$ - see front matter © 2006 Elsevier B.V. All rights reserved.
doi:10.1016/j.jorganchem.2006.07.007

potential in the synthesis of new organometallic complexes [14]. It reacts with bromothiophenol [15] and triphenylphosphine [16] to afford $[(\eta^6\text{-}C_6Me_6)_2Ru_2(SC_6H_4Br)H_2]^+$, $[(\eta^6\text{-}C_6Me_6)_2Ru_2(SC_6H_4Br)_2H]^+$ and $[(\eta^6\text{-}C_6Me_6)_2Ru_2(PPh_2)\text{-}H_2]^+$ respectively, whereupon the insertion of bridging ligands between the two ruthenium atoms implies a decrease in the metal–metal bond order and elimination of a H_2 molecule.

In this paper, we report the synthesis of two dinuclear complexes $[(\eta^6\text{-}C_6Me_6)_2Ru_2(\mu\text{-}\eta^1\text{:}\eta^2\text{-}CH\text{–}CHFc)_2(\mu\text{-}H)]^+$ (**3**) and $[(\eta^6\text{-}C_6Me_6)_2Ru_2(\mu\text{-}PPh_2)(\mu\text{-}\eta^1\text{:}\eta^2\text{-}CH\text{–}CHFc)(\mu\text{-}H)]^+$ (**4**) with σ/π-bridging ferrocenylethenyl ligands, which are obtained from the reaction of ethynylferrocene with the dinuclear precursors $[(\eta^6\text{-}C_6Me_6)_2Ru_2(\mu\text{-}H)_3]^+$ (**1**) and $[(\eta^6\text{-}C_6Me_6)_2Ru_2(\mu\text{-}PPh_2)(\mu\text{-}H)_2]^+$ (**2**), respectively, and isolated as their tetrafluoroborate salts. We present the spectroscopic characterisation and the electrochemical study of **1**–**4** as well as the single-crystal X-ray structure analysis of [**4**][BF_4].

2. Results and discussion

2.1. Synthesis and characterisation

The dinuclear cation $[(\eta^6\text{-}C_6Me_6)_2Ru_2(\mu\text{-}H)_3]^+$ (**1**) [14a,17] reacts with ethynylferrocene at 55 °C in ethanol to form $[(\eta^6\text{-}C_6Me_6)_2Ru_2(\mu\text{-}\eta^1\text{:}\eta^2\text{-}CH\text{–}CHFc)_2(\mu\text{-}H)]^+$ (**3**). The related dinuclear cation $[(\eta^6\text{-}C_6Me_6)_2Ru_2(\mu\text{-}PPh_2)(\mu\text{-}\eta^1\text{:}\eta^2\text{-}CH\text{–}CHFc)(\mu\text{-}H)]^+$ (**4**) is obtained in a similar manner from ethynylferrocene and the dinuclear precursor $[(\eta^6\text{-}C_6Me_6)_2Ru_2(\mu\text{-}PPh_2)(\mu\text{-}H)_2]^+$ (**2**), which is accessible from **1** and triphenylphosphine [16]. The formation of **3** and **4** involves a decrease in the metal–metal bond order and the reduction of the inserted ethynyl function via a hydride ligand transfer to give the σ–π-coordinated ethenyl ligand (Scheme 1).

Complexes **3** and **4** were isolated as tetrafluoroborate salts and characterised by mass and NMR spectroscopy. In the mass spectra they give, as expected, rise to the corresponding $[M+H]^+$ molecular peaks m/z at 949 and 925, respectively. However, the ^1H NMR spectra of **3** and **4** are complex due to the hindered rotation of the ferrocenyl moieties, which results in temperature-dependent molecular dynamics or even to conformational isomers.

In the case of **3**, the complexity of the ^1H NMR spectrum of **3** indicates three isomeric forms to be present in solution because of the three different hydride resonances: The hydride signals at δ_H −11.44 (s), −11.53 (s) and −12.67 (t) are presumably due to the presence of *endo*/*endo*, *exo*/*exo* and *endo*/*exo* isomers, as far as the relative orientation of the two ferrocenyl groups is concerned. It can be expected, however, that the two ethenyl ligands are coordinated transoid with respect to each other for steric reasons. For **4**, the ^1H NMR spectrum is complicated by hindered rotation of the ferrocenyl moiety, which causes a broadening of the signals (Fig. 1). At 20 °C two broad signals with several singlets in the region of the hexamethylbenzene protons are observed. Lowering the temperature to 10 °C causes the two broad signals to sharpen to give three singlets at δ_H 1.80, 2.19 and 2.25, respectively, which suggests the ferrocene unit of the ethenylferrocenyl ligand to be rotationally frozen, thus causing the non-equivalent hexamethylbenzene ligands to appear as well-defined sing-

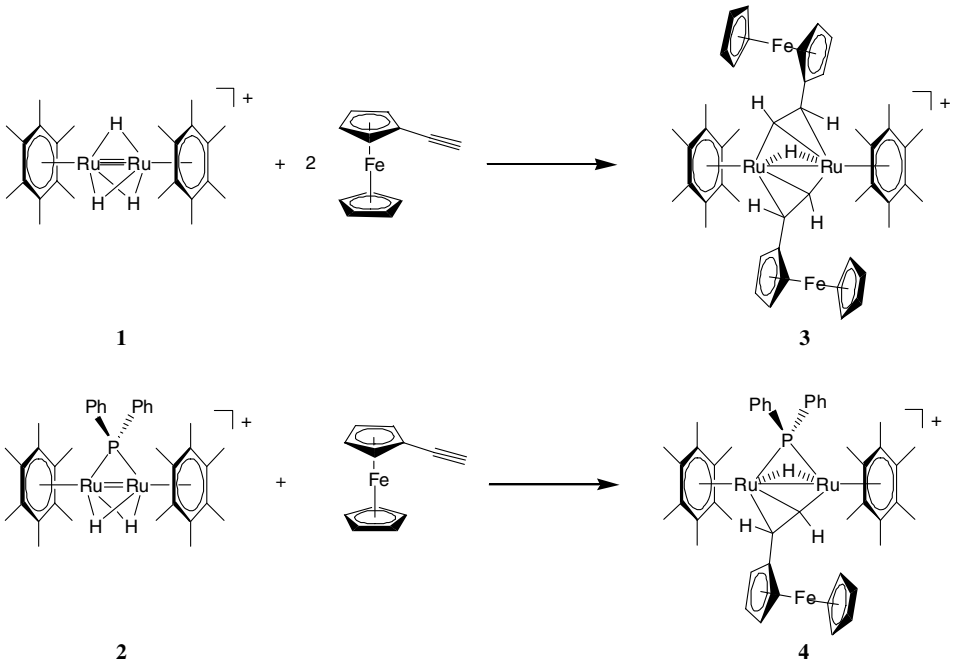

Scheme 1. ([BF_4]$^-$ anions not shown).

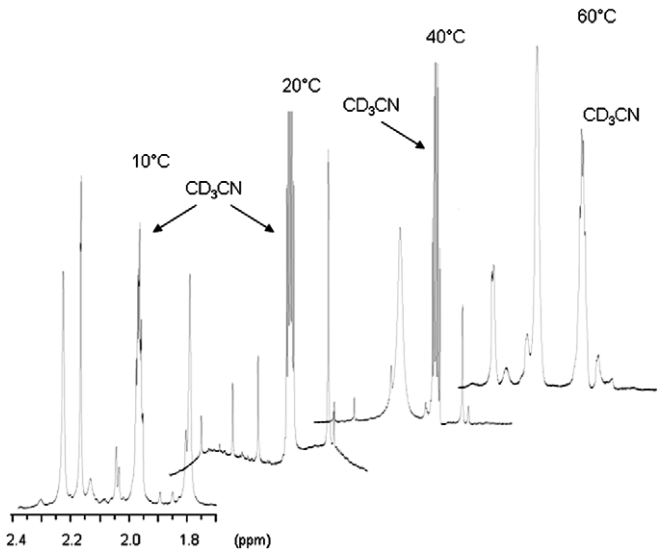

Fig. 1. Variable-temperature ^{1}H NMR spectra of **4** in CD_3CN. Only the region of the C_6Me_6 protons is shown.

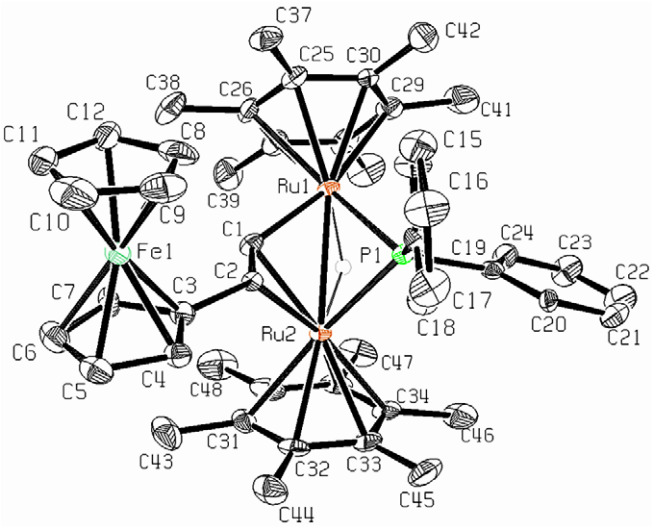

Fig. 2. ORTEP drawing of **4** at the 50% probability level with the hydrogen atoms and the tetrafluoroborate anion being omitted for clarity. Selected bond lengths (Å) and angles (°): Ru(1)–Ru(2) 2.8073(7), Ru(1)–P(1) 2.2786(17), Ru(2)–P(1) 2.3143(18), Ru(1)–C(1) 2.054(7), Ru(2)–C(1) 2.194(7), Ru(2)–C(2) 2.379(5), C(1)–C(2) 1.395(9), C(2)–C(3) 1.488(9); Ru(1)–P(1)–Ru(2) 75.35(6), Ru(1)–C(1)–Ru(2) 82.7(2), C(1)–C(2)–C(3) 121.2(6).

lets. By contrast, at 40 °C, a large singlet at δ_H 2.08 is observed for the C_6Me_6 protons, which indicates a rotation of the ferrocene moiety fast on the NMR time scale making the hexamethylbenzene ligands nearly equivalent. As expected, the C_6Me_6 signal centred at δ_H 2.08 is even sharper at 60 °C; however, other C_6Me_6 signals appear as well, indicating decomposition of **4** at this temperature.

On the other hand, the formation of complex **4** can be conveniently monitored by $^{31}P\{^{1}H\}$ NMR spectroscopy. The presence of electron donating ferrocene moiety in **4** results in an upfield shift by 7 ppm for the $^{31}P\{^{1}H\}$ NMR resonance (δ_P 105.6), as compared to complex **2** (δ_P 98.7). Notably, the ^{31}P resonance is observed as a broad singlet without any complication due to isomers.

The single-crystal X-ray diffraction analysis of [**4**][BF_4], recrystallised from a mixture of acetone and diethyl ether, reveals for cation **4** the presence of bridging hydrido, phosphido and η^1:η^2-2-(ferrocenyl)ethen-1-yl ligands coordinated to the two ruthenium atoms, which are both capped by η^6-C_6Me_6 ligands. The ethenyl ligand was found to be in the expected (*E*)-configuration for steric reasons. The formation of the ethenylferrocenyl ligand can be explained by the insertion of the C≡C unit of ferrocenylacetylene into one of the two Ru–H–Ru bridges in **2**, accompanied by the transfer of a hydrido bridge from the diruthenium backbone onto the α-carbon. The molecular structure of **4** is shown in Fig. 2.

The Ru–Ru distance [2.8073(7) Å] is within the range typical for ruthenium–ruthenium single bond [18]. The presence of a PPh_2 and an ethenylferrocenyl bridging ligands forces the arene moieties out of the coplanar arrangement, the planes of the two C_6Me_6 arene ligands being tilted by as much as 49.2(2)°. The two hydrogen atoms at the C–C bond of the ethenylferrocenyl ligand are in *trans* configuration to each other. The C–C distance is slightly elongated (1.395(9) Å) as compared to a normal C=C distance (1.34 Å) while the C(1) carbon is practically equidistant from the two ruthenium atoms. The geometry of the ferrocenylethenyl bridge compares favourably to that in other dinuclear complexes with σ–π-ethenyl derivatives [19]. The torsion angle involving the two ruthenium atoms and the coordinated vinyl unit Ru(1)–C(1)–C(2)–Ru(2) is 71.3(5)°.

2.2. Electrochemistry

The electrochemical properties of the cationic ethenylferrocenyl bridged complexes (**3** and **4**) and their parent compounds **1** and **2** were studied in the anodic region by cyclic voltammetry and voltammetry at a rotating platinum disc electrode (RDE). The data are summarised in Table 1. The first to be discussed is the electrochemical behaviour of the non-ferrocenylated precursors **1** and **2**. Complex **1** is oxidised in a single, irreversible diffusion controlled two-electron process ($E_{pa} = 0.76$ V vs. ferrocene/ferrocenium), which can be attributed to the $Ru^{II} \rightarrow Ru^{III}$ oxidation involving both metal centres, followed very likely by decomposition of the complex molecule (Fig. 3a). The anodic peak potential of the oxidation wave increases with the scan rate (v) while the peak current (i_{pa}) is directly proportional to $v^{1/2}$ and indicative of a multielectron exchange probably resulting from a reversible one-electron process being followed by a rather fast chemical reaction that, on the whole, results in a limiting, irreversible two-electron ECE mechanism (see below).

By contrast, the phosphido-bridged diruthenium(II) complex **2** undergoes two well-separated one-electron oxi-

Table 1
Summary of electrochemical data[a]

Complex	E_{pa} (V)	E_{pc} (V)	ΔE_p (mV)	$E^{0\prime}$ (V)
1	+0.76[b]	–	–	–
2	+0.22	+0.15	70	+0.19
	+0.84	+0.76	80	+0.80
3	+0.02	−0.05	70	−0.02
	+0.17	+0.09	80	+0.13
	+0.57[b]	–	–	–
4	+0.10	+0.03	70	+0.07
	+0.45	+0.37	80	+0.41
	+0.81[b]	–	–	–

[a] The potentials are given relative to ferrocene/ferrocenium reference. Potential for irreversible waves are given as obtained at scan rate of 100 mV/s. *Definitions*: $\Delta E_p = E_{pa} - E_{pc}$, $E^{0\prime} = 1/2(E_{pa} + E_{pc})$.
[b] Irreversible (or pseudoreversible) wave.

dations ($E_{pa} = 0.22$ and 0.84 V; Fig. 3b): the first oxidation is fully reversible on the cyclic voltammetric time scale, diffusion-controlled ($i_{pa}/i_{pc} \approx 1$, $i_p \propto v^{1/2}$; see also ΔE_p in Table 1) process, whereas the second one is only partially reversible. The reduction counter-peak corresponding to the second oxidation is observable only at relatively higher scan rates (above ca. 100 mV/s) and the relative height of the second anodic peak changes with the scan rate: the $i_{pa}(2)/i_{pa}(1)$ ratio increases with decreasing scan rate (cf. 1.6 at 20 mV/s and 1.2 at 200 mV/s; $i_{pa}(1)$ and $i_{pa}(2)$ denote anodic peak currents of the first and the second oxidation wave, respectively).

The presence of the ferrocenylethenyl bridges in **3** and **4** is reflected by additional reversible redox processes due to the ferrocene units. Thus, compound **3** first undergoes two successive, ferrocene-centred oxidations separated by ca. 150 mV, followed by the oxidation of the Ru–Ru core. Whereas the first ferrocene oxidation ($E_{pa} = 0.02$ V) seems to be fully reversible, the reversibility of the second one ($E_{pa} = 0.17$ V) is probably affected by the previous ferrocene oxidation. This is manifested by different heights and slopes of the voltammetric waves recorded at rotating disc electrode (RDE) [$i_{lim}(1) > i_{lim}(2)$] and further by a minor post-peak (indicated by only a 'shoulder') located about 60–70 mV more positively from the second peak in the cyclic voltammogram (Fig. 3c). The first oxidation of the Ru–Ru core of **3** follows at 0.57 V (Fig. 3c) as a diffusion-controlled one-electron process ($i_{pa} \propto v^{1/2}$). However, it is associated with a strong adsorption of the electrogenerated product. Although a fast back-scan allows the simultaneous observation of the respective reduction counter-peak and a sharp desorption peak, the latter becomes dominating after raising the switching potential (i.e. delaying the back scan) or electrolysis at a potential higher than the anodic peak potential (see Fig. 3c). The adsorption phenomena are evident also from the voltammetric curves recorded at RDE (Fig. 4a), which show, after two ill-separated sigmoidal waves due to the ferrocene oxidations, a "hump" at potentials where the last oxidation occurs. Remarkably, the adsorption does *not* affect the antecedent redox steps; the waves due to the ferrocene/ferrocenium

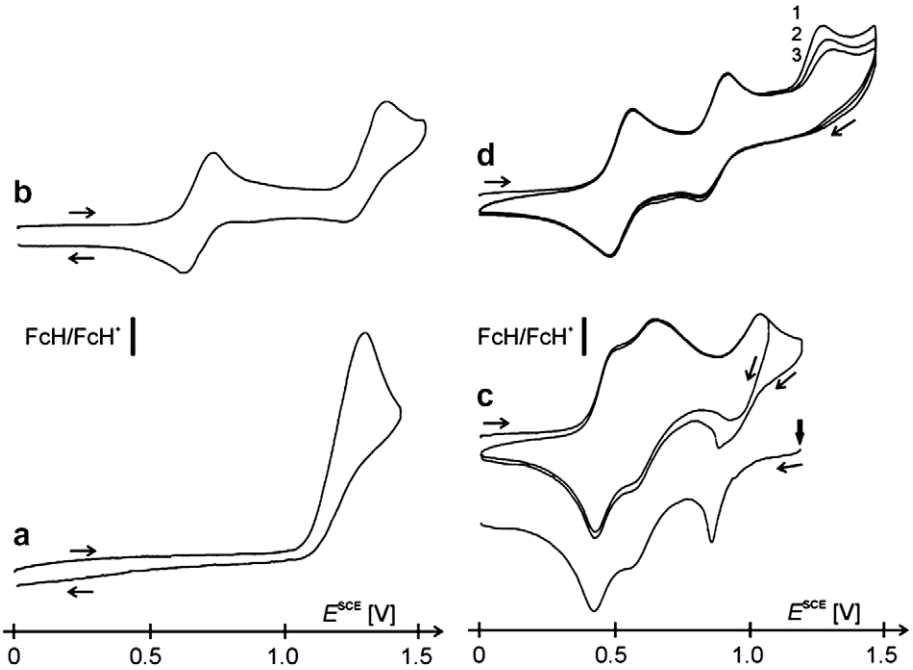

Fig. 3. Cyclic voltammograms of **1** (a), **2** (b), **3** (c), and **4** (b). The potentials are given relative to SCE while the position of the ferrocene/ferrocenium reference ($E^{0\prime} = 0.47$ V) is indicated with a bar. Note the changes in the cyclic voltammogram of **4** after increasing the switching potential (c, top) and electrolysis for 5 s at the potential indicated with the vertical arrow (c, lower trace). Conditions: ca. 5×10^{-4} M dichloromethane solutions with 0.05 M Bu_4NPF_6 supporting electrolyte, stationary platinum disc electrode, scan rate 200 mV/s.

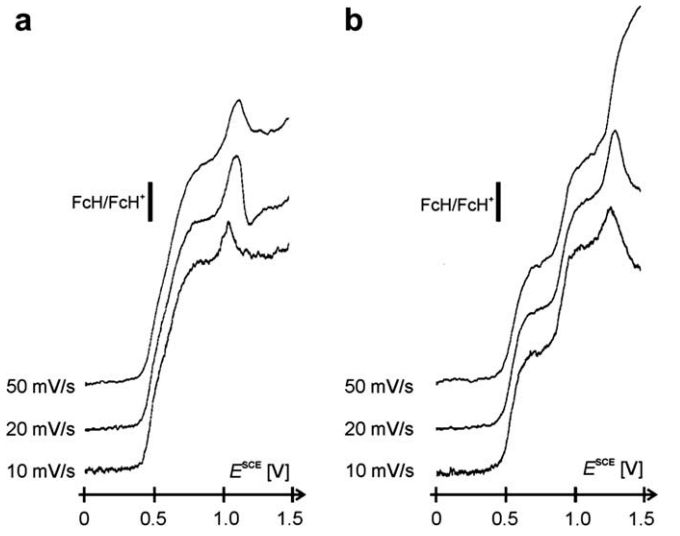

Fig. 4. Voltammetric curves recorded for **3** (a) and **4** (b) with varying scan rate (rotating platinum disc electrode (500 rpm); other conditions are as given in Fig. 3). The potential of the ferrocene/ferrocenium reference is indicated with a vertical bar.

couples are observed without any change during the back scan in cyclic voltammetry ($i_{pa}/i_{pc} \approx 1$, $i_p \propto v^{1/2}$).

The redox behaviour of **4** very much resembles that of **2** with an additional wave of the ferrocene unit at the least positive potential ($E_{pa} = 0.10$ V; Fig. 3d). All the waves are due to one-electron processes, however, whereas the first two processes assigned to ferrocene/ferrocenium and first core oxidations are reversible (i_{pa}/i_{pc} close to unity, $i_p \propto v^{1/2}$), the latter one is complicated by following chemical steps ($i_p \propto v^{1/2}$ but decreases upon repeated scanning). Similarly to **3**, voltammograms recorded at RDE exhibit two standard one-electron sigmoidal waves followed by the third one, the limiting current of which decreases due to the formation of a film at the electrode surface. Coverage of the electrode associated with the last electrochemical oxidation is a relatively slower process and does not affect the preceding redox processes, at least for the duration of the back scan in cyclic voltammetry. A normal three-wave pattern can be reached even in the voltammograms recorded at RDE by increasing the scan rate (Fig. 4b). However, the observed limiting currents on the RDE (i_{lim}) are in ca. 1:0.85:1 ratio (at 50 mV/s), pointing to some instability of the second electrogenerated product (cf. the behaviour of **3**).

Considering the structure of the complexes studied, it is likely that any redox change encompasses the whole molecules, rather than its individual part (or individual redox centre). Thus, a plausible explanation of the observed redox behaviour should consider the presence of two (η^6-arene)ruthenium(II) centres, the different nature of the ligands spanning the Ru–Ru bond (2e donor H^- vs. the 4e donors Ph_2P^- and $\{\eta^1{:}\eta^2\text{-CH–CHFc}\}^-$), and the redox activity of the ferrocene moieties in **3** and **4**. It is also noteworthy that all compounds are 36 valence electron binuclear complexes, electron removal from which would lead to their destabilisation. This is particularly the case of **1**, where the oxidation most likely results in decomposition of the dinuclear molecule. The formal two-electron oxidation can be tentatively rationalised in terms of an ECE process consisting of a primary one-electron oxidation (electrochemical step), decomposition of the electrogenerated radical (chemical step) which is associated with the second one-electron oxidation (electrochemical step).

The presence of a stronger electron-donating PPh_2 group in **2** leads to a substantial stabilisation of the dinuclear core (which can be now oxidised by two successive one-electron steps) and makes the first oxidation markedly easier and reversible. The value of $K_{com} \approx 2 \times 10^{10}$ calculated from the separation of the redox steps ($\Delta E^{0\prime} = 0.61$ V) allows one to rate **2** as a fully delocalised redox system, or class III in Robin–Day classification [20]. This supports the anticipated electronic coupling between the metal centres and the assumption that electron removal occurs from the whole bimetallic core (or perhaps even from the entire Ru_2P moiety).

Introduction of a conjugated μ–$\eta^1{:}\eta^2$-2-(ferrocenyl)-ethen-1-yl linker (**3** and **4**) can be expected to further increase electron density at the core as compared to the parent complexes and causes formal reduction of the Ru–Ru bond order. In addition, it leads to incorporation of an additional redox centre. The ferrocenyl group is known to act as a strong electron donor. However, its oxidation preceding the oxidation of the Ru–Ru core converts it into electron-deficient ferrocenium moiety and, simultaneously, increases the overall positive charge, which both should make any further electron removal more difficult.

In the case of **3**, the two ferrocene groups are oxidised prior to the oxidation of the Ru–Ru core. Nevertheless, the donating ability of the whole CH–CHFc groups seems to prevail over the reduced donor ability of the oxidised ferrocenyl moiety, causing the first core oxidation to shift negatively by ca. 0.19 V as compared to **1**. The occurrence of individual ferrocene oxidations indicates some electronic coupling even between the remote ferrocenyl moieties, the potential difference corresponding to class II in Robin–Day mixed-valence classification ($K_{com} \approx 10^2$). The potential difference for the successive core oxidations in **4** (0.36 V) is significantly lower than in **2** and may correspond to the reduced Ru–Ru bond order in the former compound. Furthermore, the ferrocene/ferrocenium oxidation which precedes the oxidation of the core in **4** is by about 80 mV less positive than the first ferrocene wave in **3**, indicating the CH–CHFc moiety to be a more powerful electron donor than the phosphido Ph_2P.

3. Experimental

3.1. General

Solvents (puriss grade) were degassed and saturated in nitrogen prior to use (not dried, if not mentioned). All manipulations were carried out under nitrogen by using standard Schlenk techniques. The dinuclear complexes,

$[(\eta^6\text{-}C_6Me_6)_2Ru_2(\mu\text{-}H)_3]^+$ (**1**) [14a,17] and $[(\eta^6\text{-}C_6Me_6)_2\text{-}Ru_2(\mu\text{-}PPh_2)(\mu\text{-}H)_2]^+$ (**2**) [16], isolated as their tetrafluoroborate salts, were synthesised as described previously. All reagents were purchased from Aldrich or Fluka and used as received. Silica gel (type G) used for preparative thin-layer chromatography was purchased from Macherey Nagel GmbH. Deuterated NMR solvents were purchased from Cambridge Isotope Laboratories, Inc. NMR spectra were recorded using a Bruker 400 MHz, and ESI mass spectra were recorded at the University of Fribourg by Prof. Titus Jenny. Microanalyses were carried out by the Laboratory of Pharmaceutical Chemistry, University of Geneva.

3.2. Synthesis of $[(\eta^6\text{-}C_6Me_6)_2Ru_2(\mu\text{-}\eta^1\text{:}\eta^2\text{-}CH\text{–}CHFc)_2(\mu\text{-}H)][BF_4]$ ([**3**][BF_4])

$[(\eta^6\text{-}C_6Me_6)_2Ru_2(\mu\text{-}H)_3][BF_4]$ (100 mg, 0.16 mmol) and ethynylferrocene (100 mg, 0.48 mmol) are dissolved in degassed puriss ethanol (20 mL) in a pressure Schlenk under nitrogen. The resulting solution is heated to 55 °C and stirred for 24 h. After 24 h, the reaction mixture is cooled to room temperature and the solvent evaporated to dryness. The brown-orange crude product is purified by preparative thin-layer chromatography on silica (eluent acetone/dichloromethane 1:10). The fraction containing the product is extracted from the orange-brown band with acetone and evaporation of the solvent gives [**3**][BF_4] (25 mg, 0.024 mmol, yield 15%) as a mixture of *endo*/*endo*, *exo*/*exo* and *endo*/*exo* isomers.

^{1}H NMR (400 MHz, [D$_6$]acetone, 25 °C): $\delta = 7.07$ (d, $J = 1.8$ Hz, *H*C–CH), 6.86 (m, *H*C–CH) 6.28 (dd, $J = 4.6$ Hz, $J = 12.5$ Hz, *H*C–CH), 6.15 (d, $J = 2.4$ Hz, *H*C–CH), 5.08 (m, *Fc*), 4.83 (m, *Fc*), 4.57–4.25 (m, *Fc*), 4.25 (s, *Fc*), 4.21 (s, *Fc*), 4.20 (s, *Fc*), 3.97 (d, $J = 12.5$ Hz, HC–C*H*), 3.87 (m, *Fc*) 2.45 (s, C$_6$*Me*$_6$), 2.43 (s, C$_6$*Me*$_6$), 2.12 (s, C$_6$*Me*$_6$), 1.96 (s, C$_6$*Me*$_6$), 1.90 (s, C$_6$*Me*$_6$), −11.44 (s, *hydride*), −11.53 (s, *hydride*), −12.67 (t, $J = 4.6$ Hz, *hydride*); MS (ESI): *m*/*z*: 949 $[M+H]^+$; Elemental analysis (%) Anal. Calc. for $C_{48}H_{59}BF_4Fe_2Ru_2$ (1036.62): C, 55.61; H, 5.74. Found: C, 55.42; H, 5.75.

3.3. Synthesis of $[(\eta^6\text{-}C_6Me_6)_2Ru_2(\mu\text{-}PPh_2)(\mu\text{-}\eta^1\text{:}\eta^2\text{-}CH\text{–}CHFc)(\mu\text{-}H)][BF_4]$ ([**4**][BF_4])

$[(\eta^6\text{-}C_6Me_6)_2Ru_2(\mu\text{-}PPh_2)(\mu\text{-}H)_2][BF_4]$ (100 mg, 0.16 mmol) and ethynylferrocene (75 mg, 0.35 mmol) are dissolved in degassed puriss ethanol (20 mL) in a pressure Schlenk under nitrogen. The resulting solution is heated to 80 °C and stirred for 24 h. After 24 h, the reaction mixture is cooled to room temperature and the solvent evaporated to dryness. The crude brown-orange product is purified by preparative thin-layer chromatography on silica (eluent acetone/dichloromethane 1:10). The fraction containing the product is extracted with acetone from the main orange-brown band and evaporation of the solvent gives [**4**][BF_4] (70 mg, 0.07 mmol, yield 43%) as a mixture of isomers (95:5). The major product (*E* isomer) is crystallised by diffusion of diethyl ether in an acetone solution containing the mixture of isomers.

^{1}H NMR (400 MHz, [D$_6$]acetone, 25 °C): $\delta = 7.67$ (m, 5H, C$_6$*H*$_5$), 7.34 (m, 3H, C$_6$H$_5$), 6.89 (m, 2H, C$_6$*H*$_5$), 6.57 (dd, 1H, $^3J_{(H,H)} = 2.8$ Hz, $^3J_{(H,H)} = 13$ Hz, *Fc*) 4.55 (dd, $^3J_{(H,H)} = 10.7$ Hz, $^3J_{(H,H)} = 13$ Hz, 1H, *Fc*), 4.23 (m, 2H, 3*Fc*), 3.89 (s, 5H, *Fc*), 2.5–1.8 (broad, 38H, *H*C–C*H*, C$_6$Me$_6$), −14.38 (dd, 2H, $^2J_{(H,P)} = 40$ Hz, $^3J_{(H,H)} = 3$ Hz, hydride); ^{13}C NMR (100 MHz, [D$_6$]acetone, 25 °C): $\delta =$ 140.59 (Fc-*C*H–C), 135.64 (P(C$_6$H$_5$)$_2$), 135.55 (P(C$_6$H$_5$)$_2$), 133.63 (P(C$_6$H$_5$)$_2$), 133.38 (P(C$_6$H$_5$)$_2$), 133.35 (P(C$_6$H$_5$)$_2$), 133.24 (P(C$_6$H$_5$)$_2$), 131.10 (Fc-CH–*C*) 130.00 (P(C$_6$H$_5$)$_2$), 129.97 (P(C$_6$H$_5$)$_2$), 128.65 (P(C$_6$H$_5$)$_2$), 128.56 (P(C$_6$H$_5$)$_2$), 128.32 (P(C$_6$H$_5$)$_2$), 128.21 (P(C$_6$H$_5$)$_2$), 101.78 (C$_6$Me$_6$) 98.75 (*Fc*), 85.85 (*Fc*), 69.74 (*Fc*), 69.08 (*Fc*), 16.60–17.50 (broad, C$_6$*Me*$_6$); ^{31}P{^{1}H} NMR (160 MHz, [D$_6$]acetone, 25 °C): $\delta = 105.60$ (s); MS (ESI): *m*/*z*: 925 $[M+H]^+$; Elemental analysis (%) Anal. Calc. for $C_{48}H_{58}BF_4FePRu_2$ (1010.17): C, 57.04; H; 5.78. Found: C, 57.32; H, 6.04.

3.4. Electrochemistry

Electrochemical measurements were carried out with a multipurpose polarograph PA3 interfaced to a Model 4103 XY recorded (both Laboratorní přístroje, Prague) at room temperature using a standard three-electrode cell: rotating or stationary platinum disc (1 mm diameter) working electrode, platinum wire auxiliary electrode, and saturated calomel electrode (SCE) reference electrode, separated from the analysed solution by a salt bridge filled with 0.05 M Bu_4NPF_6 in dichloromethane. The samples were dissolved in dichloromethane (Merck p.a., dried over CaH_2) to give ca. 5×10^{-4} M concentration of the analyte and 0.05 M Bu_4NPF_6 (supporting electrolyte; Fluka, puriss. for electrochemistry). The samples were degassed with argon prior to the measurement and then kept under an argon blanket. Cyclic voltammograms were recorded at stationary platinum disc electrode (scan rates 50–500 mV/s), whereas the voltammograms were obtained at rotating disc electrode (500 rpm, scan rates 10–100 mV/s). Redox potential given in Table 1 and text are given relative to ferrocene/ferrocenium reference whilst Figs. 3 and 4 show the curves "as recorded" – i.e., with the SCE reference.

3.5. Structure determination

X-ray data for [**4**][BF_4]; $C_{48}H_{58}BF_4FePRu_2$, $M =$ 1010.71 g mol^{-1}, monoclinic, $P2_1$ (no. 4), $a = 11.3508(12)$, $b = 17.7424(15)$, $c = 11.6461(13)$ Å, $\beta = 115.560(12)°$, $U =$ 2115.9(4) Å^3, $T = 173$ K, $Z = 2$, μ (Mo Kα) = 1.132 mm^{-1}, 7718 reflections measured, 7193 unique ($R_{int} = 0.1021$) which were used in all calculations. The final wR (F^2) was 0.1474 (all data). The data were measured using a Stoe Image Plate Diffraction system equipped with a ϕ circle, using Mo Kα graphite monochromated radiation ($\lambda =$

0.71073 Å) with ϕ range 0–200°, increment of 1.2°, 3 min per frame, 2θ range from 2.0–26°, D_{max}–D_{min} = 12.45–0.81 Å. The structure was solved by direct methods using the program SHELXS-97 [21]. The refinement and all further calculations were carried out using SHELXL-97 [22]. The H-atoms were included in calculated positions and treated as riding atoms using the SHELXL default parameters. The non-H atoms were refined anisotropically, using weighted full-matrix least-square on F^2. Fig. 2 is drawn with ORTEP [23].

Acknowledgements

The authors are grateful to the Fonds National Suisse de la Recherche Scientifique and the Ministry of Education, Youth and Sports of the Czech Republic for financial support. A generous loan of ruthenium chloride hydrate from the Johnson Matthey Technology Centre is gratefully acknowledged.

Appendix A. Supplementary data

CCDC-606629 [**4**][BF_4] contains the supplementary crystallographic data for this paper. These data can be obtained free of charge at www.ccdc.cam.ac.uk/conts/retrieving.html [or from the Cambridge Crystallographic Data Centre, 12, Union Road, Cambridge CB2 1EZ, UK, fax: (int.) +44 1223 336 033, e-mail: deposit@ccdc.cam.ac.uk]. Supplementary data associated with this article can be found, in the online version, at doi:10.1016/j.jorganchem.2006.07.007.

References

[1] (a) G.E. Rodgers, W.R. Cullen, B.R. James, Can. J. Chem. 61 (1983) 1314–1318;
(b) D. Pilette, K. Ouzzine, H. Le Bozec, P.H. Dixneuf, C.E.F. Rickard, W.R. Roper, Organometallics 11 (1992) 809–817;
(c) H. Le Bozec, D. Pilette, P. Dixneuf, New J. Chem. 14 (1990) 793–794;
(d) M. Sato, M. Sekino, J. Organomet. Chem. 444 (1993) 185–190;
(e) A. Marinetti, F. Labrue, B. Pons, S. Jus, L. Ricard, J.-P. Genêt, Eur. J. Inorg. Chem. (2003) 2583–2590;
(f) P. Barbaro, C. Bianchini, G. Giambastiani, A. Togni, Eur. J. Inorg. Chem. (2003) 4166–4172;
(g) S. Gischig, A. Togni, Organometallics 23 (2004) 2479–2487;
(h) S. Pavlik, K. Mereiter, M. Puchberger, K. Kirchner, J. Organomet. Chem. 690 (2005) 5497–5507;
(i) S.-I. Fukuzawa, T. Suzuki, Eur. J. Org. Chem. (2006) 1012–1016.
[2] (a) N. Dowling, P.M. Henry, N.A. Lewis, H. Taube, Inorg. Chem. 20 (1981) 2345–2348;
(b) Y. Kasahara, Y. Hoshino, M. Kajitani, K. Shimizu, G.P. Satô, Organometallics 11 (1992) 1968–1971;
(c) J.-C. Chambron, C. Coudret, J.-P. Sauvage, New J. Chem. 16 (1992) 361–367;
(d) M. Sato, H. Shintate, Y. Kawata, M. Sekino, Organometallics 13 (1994) 1956–1962;
(e) M.C.B. Colbert, S.L. Ingham, J. Lewis, N.J. Long, P.R. Raithby, J. Chem. Soc. Dalton Trans. (1994) 2215–2216;
(f) C. Lebreton, D. Touchard, L. Le Pichon, A. Daridor, L. Toupet, P.H. Dixneuf, Inorg. Chim. Acta 272 (1998) 188–196;
(g) V. Mamane, A. Gref, O. Riant, New J. Chem. 28 (2004) 585–594;
(h) T.J. Burchell, I.W. Wyman, K.N. Robertson, T.S. Cameron, M.A.S. Aquino, Organometallics 23 (2004) 5353–5364;
(i) A. Klein, O. Lavastre, J. Fiedler, Organometallics 25 (2006) 635–643.
[3] (a) M. Buchmeiser, H. Schottenberger, Organometallics 12 (1993) 2472–2477;
(b) N.D. Jones, M.O. Wolf, D.M. Giaquinta, Organometallics 16 (1997) 1352–1354;
(c) M. Uno, P.H. Dixneuf, Angew. Chem., Intl. Ed. 37 (1998) 1714–1717;
(d) O. Briel, A. Fehn, K. Polborn, W. Beck, Polyhedron 18 (1999) 225–242;
(e) U. Behrens, T. Meyer-Friedrichsen, J. Heck, Z. Anorg. Allg. Chem. 629 (2003) 1421–1430;
(f) P. Yuan, S. Hua Liu, W. Xiong, J. Yin, G. Yu, H. Yung Sung, I.D. Williams, G. Jia, Organometallics 24 (2005) 1452–1457;
(g) T.-Y. Dong, K. Chen, M.-C. Lin, L. Lee, Organometallics 24 (2005) 4198–4206;
(h) M. Malessa, J. Heck, J. Kopf, M.H. Garcia, Eur. J. Inorg. Chem. (2006) 857–867.
[4] A. Carella, G. Rapenne, J.-P. Launay, New J. Chem. 29 (2005) 288–290.
[5] (a) M.W. Cooke, C.A. Murphy, T. Stanley Cameron, J.C. Swarts, M.A.S. Aquino, Inorg. Chem. Commun. 3 (2000) 721–725;
(b) M.W. Cooke, C.T. Stanley Cameron, K.N. Robertson, J.C. Swarts, M.A.S. Aquino, Organometallics 21 (2002) 5962–5971.
[6] M. Auzias, B. Therrien, G. Labat, H. Stoeckli-Evans, G. Süss-Fink, Inorg. Chim. Acta 359 (2005) 1012.
[7] B. Therrien, L. Vieille-Petit, J. Jeanneret-Gris, P. Štěpnička, G. Süss-Fink, J. Organomet. Chem. 689 (2004) 2456–2463.
[8] G.-L. Xu, M.C. DeRosa, R.J. Crutchley, T. Ren, J. Am. Chem. Soc. 126 (2004) 3728–3729.
[9] (a) W.-Z. Chen, T. Ren, Organometallics 23 (2004) 3766–3768;
(b) W.-Z. Chen, T. Ren, Organometallics 24 (2005) 2660–2669.
[10] G.-L. Xu, R.J. Crutchley, M.C. DeRosa, Q.-J. Pan, H.-X. Zhang, X. Wang, T. Ren, J. Am. Chem. Soc. 127 (2005) 13354–13363.
[11] M.I. Bruce, P.J. Low, F. Hartl, P.A. Humphrey, F. de Montigny, M. Jevric, C. Lapinte, G.J. Perkins, R.L. Roberts, B.W. Skelton, A.H. White, Organometallics 24 (2005) 5241–5255.
[12] S. Takemoto, S. Kuwata, Y. Nishibayashi, M. Hidai, Organometallics 19 (2000) 3249–3252.
[13] R.A. Benkeser, W.P. Fitzgerald Jr., J. Org. Chem. 26 (1961) 4179–4180.
[14] (a) M. Jahncke, G. Meister, G. Rheinwald, H. Stoeckli-Evans, G. Süss-Fink, Organometallics 16 (1997) 1137–1143;
(b) M. Jahncke, A. Neels, H. Stoeckli-Evans, G. Süss-Fink, J. Organomet. Chem. 561 (1998) 227–235;
(c) M. Jahncke, A. Neels, H. Stoeckli-Evans, G. Süss-Fink, J. Organomet. Chem. 565 (1998) 97–103;
(d) M. Faure, M. Jahncke, A. Neels, H. Stoeckli-Evans, G. Süss-Fink, Polyhedron 18 (1999) 2679–2685;
(e) L. Vieille-Petit, B. Therrien, G. Süss-Fink, Inorg. Chem. Commun. 7 (2004) 232–234.
[15] M.J.-L. Tschan, F. Chérioux, B. Therrien, G. Süss-Fink, Eur. J. Inorg. Chem. (2004) 2405–2411.
[16] M.J.-L. Tschan, F. Chérioux, L. Karmazin-Brelot, G. Süss-Fink, Organometallics 24 (2005) 1974–1981.
[17] (a) M.A. Bennett, J.P. Ennett, K.I. Gell, J. Organomet. Chem. 233 (1982) C17–C20;
(b) M.A. Bennett, J.P. Ennett, Inorg. Chim. Acta 198-200 (1992) 583–592.
[18] S.K. Patra, N. Sadhukhan, J.K. Bera, Inorg. Chem. 45 (2006) 4007–4015.
[19] M. Akita, R. Hua, S.A.R. Knox, Y. Moro-oka, S. Nakanishi, M.I. Yates, J. Organomet. Chem. 569 (1998) 71–83.

[20] (a) M.C. Robin, P. Day, Adv. Inorg. Chem. Radiochem. 10 (1967) 247; (b) P. Zanello, Inorganic Electrochemistry–Theory, Practice and Application, RSC, Cambridge United Kingdom, 2003 (Chapter 2, Section 1.5, p. 99 and Chapter 4, Section 1.3, p. 171).
[21] G.M. Sheldrick, Acta Crystallogr., Sect. A 46 (1990) 467.
[22] G.M. Sheldrick, SHELXL-97, University of Göttingen, Göttingen, Germany, 1999.
[23] L.J. Farrugia, J. Appl. Cryst. 30 (1997) 565.